Biodegradable jute cloth reinforced thermoplastic copolyester composites: fracture and failure behaviour

B. A. Acha[1], N. E. Marcovich[2] and J. Karger-Kocsis*[1]

Jute cloth reinforced, fully biodegradable thermoplastic composites were produced by the film stacking technique, with a semicrystalline copolyester (Ecoflex) as the matrix material. The jute cloth content varied between 0, 20 and 40 wt-% in the sheets produced by hot pressing. Specimens cut from the sheets were subjected to in plane static and out of plane dynamic loading, and the related fracture and failure behaviours were studied. The jute cloth proved to be a useful reinforcement to enhance in plane mechanical properties. The *J* integral concept (*J–R* curve) was adopted to assess the fracture behaviour of the composites. Crack propagation in single edge notched tensile (SEN-T) loaded specimens was detected using position resolved acoustic emission (AE). Acoustic emission was also used to characterise the failure. Surprisingly, no beneficial effect of the jute cloth was observed in the out of plane, namely instrumented falling weight impact (IFWI) test. This could be explained by the characteristics of the jute cloth used (the large mesh size increases the tendency to disintegrate when stretched at high strain rates) and by its moderate adhesion toward the matrix.

Keywords: Biocomposite, Jute, Film stacking, Fracture, Failure, Acoustic emission, J integral, Perforation impact, Ecoflex

Introduction

Increased resistance to environmental effects is a frequent objective of research and development of polymers and their related composites. On the other hand, there are numerous applications in which environmental degradation of the products is beneficial. These are driven, for example, by the seasonal use of polymers (e.g. in agriculture and horticulture), and more generally, by solving the end of life 'recycling' issues in a straightforward way. Growing environmental consciousness,[1] new rules and regulations throughout the world are forcing polymer producers to consider ecofriendly products the production of which is challenging.[2]

The use of renewable material resources has to date been restricted to natural fibres. These are used as reinforcements in various synthetic polymers.[3–7] Such biofibre based composites meet most property (especially mechanical characteristics) requirements although some biodegradability issues remain. On the other hand, by embedding natural fibres into biodegradable polymeric matrices, 'real biocomposites' can be produced.

The matrix of such biocomposites can be derived from naturally renewable resources, or be produced from synthetic monomers.[8] The biodegradable thermoplastic polyester, Ecoflex, manufactured by BASF, is a semicrystalline copolyester produced by polycondensation of butyleneglycol, terephthalic acid and adipic acid. Its melting range (at ~110°C) and mechanical properties are both similar to those of polyethylenes. As a consequence, Ecoflex is a candidate material for packaging and especially for agricultural use (mulch films, greenhouse covering films and the like).

Among all the natural reinforcing materials, jute is one of the most common agrofibres with high tensile modulus and low elongation at break. If its low density (1·45 g cm^{-3}) is taken into consideration, its specific stiffness and strength are comparable with the respective values of glass fibre.[9–12] The specific (i.e. density related) modulus of jute is higher than that of glass fibre and based on the calculation of modulus per cost, jute is far superior to glass reinforcements. The specific strength per unit cost of jute approaches that of glass fibres. There are many reports about the use of jute as the reinforcement in both thermosets[13–16] and thermoplastics.[12,17,18] Mohanty and Misra[19] have reviewed jute reinforced thermoset, thermoplastic and rubber based composites. Less attention was paid, however, to the jute reinforcement in biodegradable matrices.[20,21]

The present paper reports a study on the effect of jute cloth content on the in plane and out of plane fracture behaviour of biocomposites containing an Ecoflex grade as the matrix. A further purpose of this work was to determine the fracture and failure behaviour of these

[1]Institut für Verbundwerkstoffe GmbH (Institute for Composite Materials), Kaiserslautern University of Technology, D–67663 Kaiserslautern, Germany
[2]Institute of Materials Science and Technology (INTEMA), University of Mar del Plata, 7600 Mar del Plata, Argentina

*Corresponding author, email karger@ivw.uni-kl.de

Published by Maney on behalf of the Institute
Received 24 August 2005; accepted 21 February 2006
DOI 10.1179/174328906X79978

composites by adopting the acoustic emission (AE) technique.

Experimental

Materials

Commercial bidirectional jute fabrics (plain weave 0/90; with the same amount of roving in the weft and warp directions) were used as the reinforcement layers. Volumetric and surface densities of the fabrics were $0{\cdot}464 \pm 0{\cdot}05$ g cm^{-3} and $0{\cdot}027 \pm 0{\cdot}002$ g /cm^{-2} respectively. The fibre linear density of the jute (which is a measure of the average number of fibres in the cross-section of a given yarn) was 310 ± 60 tex.

A biodegradable polymer, Ecoflex FBX 7011, kindly supplied by BASF (Ludwigshafen, Germany), was used as the matrix. Ecoflex FBX 7011 is a biodegradable copolyester based on monomers 1,4-butanediol, adipic acid and terephthalic acid. The basic properties of this polymer are summarised in Table 1.

Composite preparation

Fabrication of the composites consists of two steps. In the first step, Ecoflex films with different thickness, approximately 0·3 and 0·5 mm, were prepared by compression moulding using a hydraulic press (Type PMC 2SP, Satim SA, France) at 150°C (reflecting the melting of Ecoflex) under 25 bar pressure.

In the second step, composite sheets were produced by the film stacking technique. Accordingly, a given number of jute cloths were sandwiched in between the polymer films before hot pressing. Composites with 20 and 40 wt-% jute content (nominal values) were prepared. Depending on the reinforcement amount for each composite sheet, matrix films with different thicknesses and numbers were selected. The composite sheets were compression moulded at 150°C under 25 bar for 20 min. The jute fabric was dried at 70°C for 30 min before hot pressing. It should be mentioned here that film stacking will be an economic process only when performed continuously, e.g. using a double belt press as in the established technique for production of glass mat reinforced thermoplastic polypropylenes (GMT PP).

Tests

Dynamic mechanical thermal analysis (DMTA)

Viscoelastic properties, such as storage modulus E', loss modulus E'' and mechanical loss factor tan δ, as a function of temperature were measured in a DMTA device (Eplexor 150N, Gabo Qualimeter, Ahlden, Germany). The tests were carried out in a tensile mode using a rectangular specimen of $50 \times 10 \times 3$ mm (length × width × thickness) over a temperature range of −100–110°C. The samples were scanned at a heating rate 1 K min^{-1} under the nitrogen flow using a fixed frequency of 10 Hz. The static and dynamic loads were 10 and ±5 N respectively.

Table 1 Basic material properties of Ecoflex FBX 7011

Property	Value
Mass density, g cm^{-3}	1·25–1·27
Mel flow rate, g/10 min at 190°C	2·7–4·9
Melting point, °C	110–120
Shore D hardness	32
Vicat VST A/50, °C	80

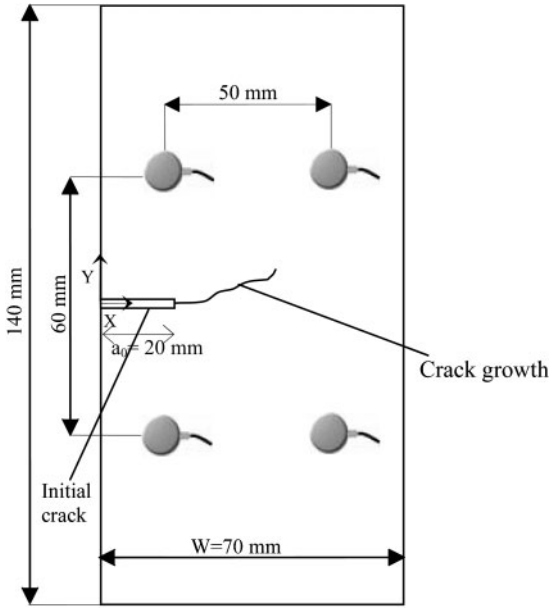

1 Experimental set-up including dimension of SEN-T specimen and positioning of AE sensors

In plane mechanical and fracture mechanical tests

Static tensile tests were performed on dumbbells cut from the plates. The width of these dumbbells was 20 mm (modified type 1B specimen according to the DIN EN ISO 527-2 standard). This allows us to determine reliable tensile mechanical data because the size of the damage zone in such composites may reach 20 mm (Ref. 22). Their loading occurred on a Zwick machine 1474 at room temperature and 5 mm min^{-1} crosshead speed. At least five specimens of each composite were tested to obtain the average value. The modulus was determined by using an incremental mechanical extensometer. In order to obtain information about the failure mode, the AE activity was registered using a microphone during loading of the specimens.

To trace the damage development, static mechanical tests were also performed on single edge notched tensile (SEN-T) loaded specimens. The notch a_0 was initially sawn and then sharpened by razor blade tapping. Tensile loading of the SEN-T loaded specimens (two specimens of each composite were tested) occurred under the same conditions as for the dumbbells. Force *v.* displacement curves were recorded during the tests. The damage zone was estimated by location of the AE events, collected during loading of the SEN-T loaded specimens. The AE activity was monitored *in situ* by a Defektophone NEZ 220 device (AEKI, Budapest, Hungary). A four sensor quadratic array was used to locate AE events using wide bandwidth (100–600 kHz) microsensors (Micro 30D of Physical Acoustic Co., Princeton, USA). Locations were determined by a built-in algorithm that required knowledge of the acoustic wave speed. The mean wave speed increased with the jute cloth content, being 600 and 1100 m s^{-1} with 20 and 40 wt-% jute reinforcement respectively.

To estimate the size of the damage zone, a mathematical weighing procedure, described elsewhere,[23,24] was used. Briefly, the located map (cf. Fig. 1) was scanned by

a circle of 6 mm diameter in 1 mm steps in both x and y directions, and for each surface point, the value in z direction was determined by a bell type weighing function. This procedure was applied to cumulative AE amplitudes. The damage zone was assigned to the surface that contained 90% of all the located AE events. The located AE events were used to trace crack growth as well, by considering movement of the centre of gravity of the cumulative AE amplitudes in subsequent time intervals. The related procedure is described in detail in Ref. 24. The percentage of the located events within the circle was considered for each surface point in the z direction, resulting in two- or three-dimensional contour plots.

The fracture surfaces of the specimens were studied with a Jeol 5300 (Tokyo, Japan) scanning electron microscope. The surface was previously coated with gold to avoid charging under the electron beam.

Out of plane tests

The perforation impact properties of the jute cloth reinforced composites were also evaluated. Instrumented falling weight impact (IFWI) tests were carried out using a Dartvis tower (Ceast, Pianezza, Italy) at −30°C, room temperature and 80°C. The samples (60 × 60 mm), clamped on a supporting ring of 40 mm diameter, were impacted with a hemispherically tipped dart (20 mm in diameter; impactor mass of 23·357 kg) at an incident speed of 4·4 m s^{-1}. At least four plates for each material were impacted.

From the IFWI fractograms, the thickness related maximum force (F_{max}/t), the thickness related energy at maximum load (E_{max}/t) and at perforation (E_{perf}/t) as well as the ductility index (DI) were determined. The latter parameter is given by equation (1)

$$DI = \frac{E_{perf} - E_{max}}{E_{perf}} \quad (1)$$

Results and discussion

DMTA behaviour

The storage modulus E' is a measurement of the load bearing capacity of the material and is analogous to tensile modulus E. The variation of E' as a function of temperature for samples with different fibre content (0, 20 and 40 wt-%) is presented in Fig. 2. It is evident that the incorporation of jute increases the modulus of the corresponding composites in the whole temperature range. E' decreased with increasing temperature and exhibited a significant fall between −38 and −10°C. This change is linked to the glass transition temperature T_g of the copolyester matrix. Note that beyond T_g, E' values of the composites are much higher than that of the pure matrix. This behaviour is primarily attributed to the reinforcing effect of the jute fabric. As expected, the difference in E' moduli between the glassy and rubbery states is smaller for the composites than for the neat polymer. This can be attributed to the mechanical constraint introduced by the reinforcement at high concentrations, which reduce the chain mobility and therefore the deformability of the matrix.

With increasing temperature, the benefits of the natural fibre reinforcement become even more obvious. The increasing mobility of the macromolecules is

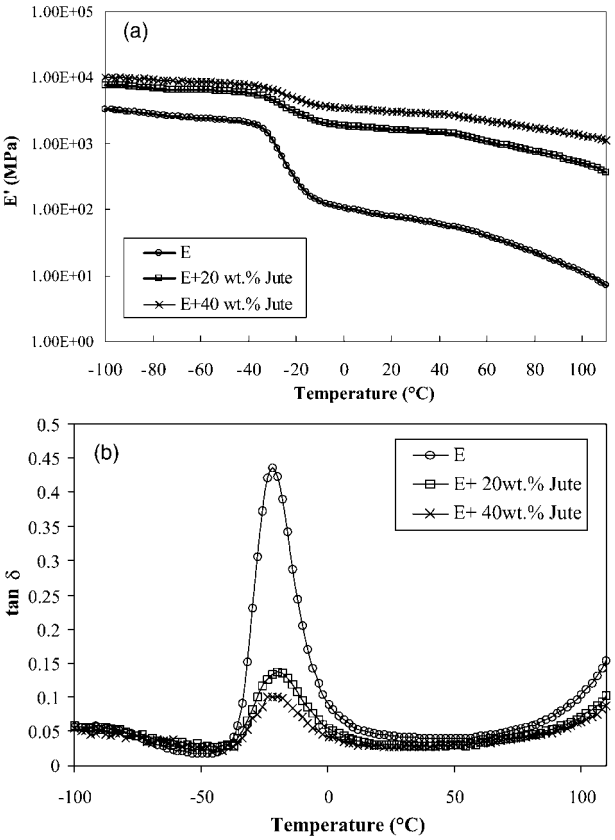

2 *a* curves of storage modulus E' and *b* tan δ versus temperature for plain Ecoflex E and its jute cloth reinforced composites at various jute content

counteracted by the reinforcing fibres. This, for example, leads at 40°C to an increase in the modulus from 60 to 1470 MPa (with 20 wt-% jute) and to 2800 MPa (with 40 wt-% jute). Similar observations with respect to the DMTA properties were reported for other natural fibre reinforced polymer composites.[25,26] However, when using short natural fibres[27–29] instead of fabrics, the stiffness increment was not so pronounced. Below T_g, the same changes in the storage moduli are observed as a function of jute content as above T_g, but in a markedly reduced extent. This is because the stiffness is controlled primarily by the strength of the intermolecular forces and the way the polymer chains is packed.[28] Accordingly, the matrix contribution to the stiffness of the composites below T_g is larger than that beyond T_g of the matrix.

The effectiveness of fillers on the modulus of the composites can be quantified by a coefficient C based on Ref. 30

$$C = \frac{(E_g'/E_r')_{comp}}{(E_g'/E_r')_{resin}} \quad (2)$$

where E_g' and E_r' are the storage moduli in the glassy and rubbery states respectively. The higher the C value, the lower the effectiveness of the filler. The measured E' values at −80 and 40°C were considered as E_g' and E_r respectively. The C values obtained for 20 and 40 wt-% jute reinforcement are 0·28 and 0·07 respectively. This indicates that the effectiveness of the jute increases with its content, confirming the advantage of using jute fabrics as the reinforcement.

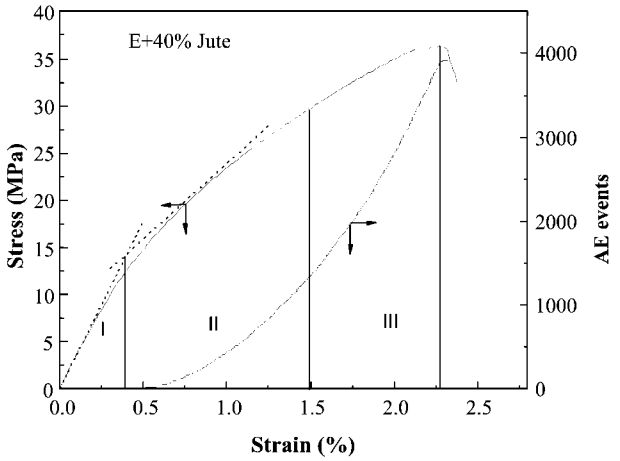

3 Stress and cumulative number of AE events as function of strain for dumbbell specimen from composite with 40 wt-% jute cloth content: load ranges used for detailed AE analysis are shown as I, II and III (*see* Fig. 4)

Figure 2*b* shows the change of tan δ as a function of temperature for pure Ecoflex and its corresponding jute composites. The neat polymer has a T_g at $-22^{\circ}C$. Between these composites, no significant difference in T_g values was detected. This suggests that the degree of interaction between the jute reinforcement and the matrix was not strong enough to alter the molecular movements. Similar behaviour has been reported by other researchers.[31] Moreover, with increasing fibre content, the area under the tan δ curve becomes smaller because the polymer content is decreased owing to the jute reinforcement, and only the amorphous phase of the matrix is involved in the glass transition.

In plane response

Tensile fracture and failure

Results obtained in the tensile tests of dumbbell specimens are listed in Table 2. It can be seen that an increase in jute cloth content is accompanied by an increase in the tensile strength and in the *E* modulus. This is due to the high strength and modulus of the jute fibres ($19{\cdot}26 \pm 4{\cdot}61$ GPa). On the other hand, the jute reinforcement reduces significantly the ultimate elongation. This decrease is due to the restriction imposed to the deformation of the matrix by jute fibres, which are less ductile than the matrix.

Figure 3 shows the cumulative number of AE events and the stress as a function of strain on the example of a dumbbell cut of the composite containing 40 wt-% jute cloth. No acoustic events could be detected during the tensile test of the pure matrix, which is acoustically inactive because of its rubber-like behaviour. It can be observed that AE starts after a certain level of loading of the dumbbell. Note that the load ranges (I, II and III) shown in Fig. 3 have been used for a more detailed AE analysis. The relative amplitude distributions of the AE events in the ranges II and III are depicted in Fig. 4.

Figure 4 clearly shows that in range II, low amplitude (20–35 dB) AE events dominate and no difference can be observed between the composites containing 20 and 40 wt-% jute respectively. For the composite with 40 wt-% jute content, with increasing load (i.e. range II), two peaks appear at higher amplitudes (about 25 and 35 dB). These are less well resolved at 20 wt-% jute content (cf. Fig. 4). It should be noted that the AE amplitude increases according to the following ranking: debonding<fibre pull-out<fibre fracture. Therefore with increasing jute content, pull-out events seem to become more dominant. This suggests that the wetting of the jute cloth is less good at high reinforcement content than at the lower content. This suggestion is in agreement with the tensile mechanical data which showed that the reinforcing effect of jute was not linear as a function of its content (cf. Table 2).

Damage development and growth

Recall that the damage zone was estimated by considering the located cumulative AE amplitudes, as described in detail in Ref. 24.

Figure 5*a* shows the characteristic force–elongation trace for a SEN-T loaded specimen cut of the composite reinforced with 20 wt-% jute cloth. Before the load maximum, several load drops ('pop ins') were observed. This phenomenon is usually an indication of crack bifurcation, during which a former satellite crack becomes dominant.[32] The appearance of the 'pop in' suggests that crack growth had started before the maximum load was reached. This is supported by the three-dimensional contour plots (cf. Fig. 5*b*) which reflect the size of the damage zone and its movement along the free ligament. It can be seen that the crack travelled from the initial notch tip already in position 1 (cf. Fig. 5*a*). On the other hand, the crack only slightly moved between positions 1 and 2, irrespective of the large load drop in between. The estimated size of the damage zone was ~8 mm, which remained fairly constant during the crack growth (cf. Fig. 5*b*).

The scenario is completely different for the composite reinforced with 40 wt-% jute. The first difference is that the load maximum is greater compared with the 20 wt-% jute composite (cf. Fig. 6*a*). The second and most prominent difference is related to the damage zone and its movement (cf. Figs. 5*b* and 6*b*). The size of the damage zone is more elliptical in shape with short (in loading direction) and long (along the ligament) diameters of about 9 and 13 mm. The weight centre point of the located AE amplitudes is just at the initial notch root. As a consequence, the crack did not grow at position 1 (cf. Fig. 6*b*). On the other hand, at position 2 the crack already passed a large part of the free ligament (cf. Fig. 6*a* and *b*). It is worth noting that the damage zone size here was larger than 10 mm, which is the width of standardised dumbbell specimens, hence the decision to use dumbbells wider than those indicated by the

Table 2 Tensile characteristics of neat Ecoflex and its composites at different jute content

Designations indicating jute content, wt-%	*E* modulus, MPa	Tensile strength, MPa	Elongation at break, %
E	$54{\cdot}52 \pm 0{\cdot}87$	$13{\cdot}47 \pm 0{\cdot}24$	$356{\cdot}7 \pm 3{\cdot}04$
E+20	$1376{\cdot}30 \pm 55{\cdot}97$	$22{\cdot}27 \pm 0{\cdot}42$	$2{\cdot}75 \pm 0{\cdot}04$
E+40	$3437{\cdot}04 \pm 99{\cdot}05$	$35{\cdot}91 \pm 0{\cdot}54$	$1{\cdot}97 \pm 0{\cdot}47$

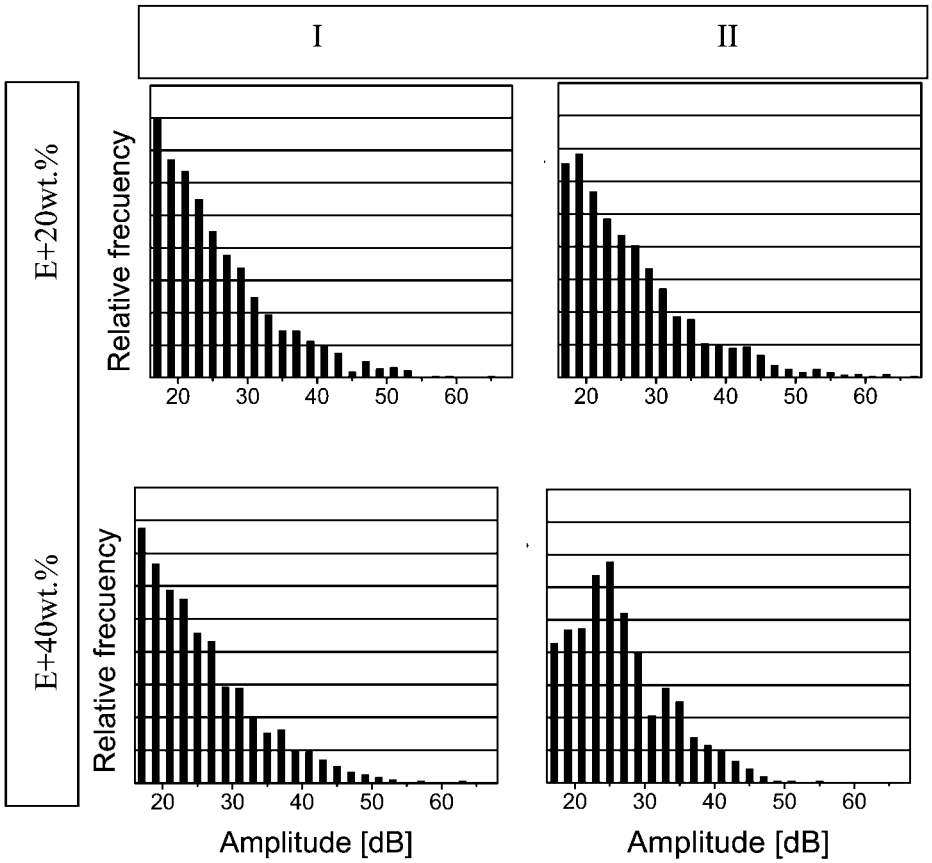

4 Characteristic AE amplitude histograms for dumbbell specimens with 20 and 40 wt-% jute reinforcements in load ranges I and II (*see* Fig. 3)

corresponding standard when determining the tensile characteristics (cf. Table 2).

Failure

Microphotographs taken from the fracture surface of the SEN-T loaded specimens (Fig. 7) show that the matrix failed in a ductile manner. However, the matrix ductility was reduced by increasing the amount of the jute cloth, as can be seen by the reduced length of the broken matrix strands (Fig. 7).

Scanning electron microscopy pictures (Fig. 8) indicate that the matrix failure is due to the breakage of elongated strands. They are formed by easy debonding from the jute fibre via subsequent stretching before the final fracture. Debonding is strongly favoured by the relative high Poisson number of Ecoflex compared with jute along with a moderate adhesion/wetting between them. This was well resolved by the AE results, as illustrated in Figs. 4 and 7.

Fracture mechanics

The very ductile failure of the composites forced us to use the J integral concept to derive reliable fracture mechanical data. The related resistance curve (J–R) approach was chosen to obtain information about the tearing modulus which is a measure of the resistance to crack propagation. This necessitates, however, knowledge of the crack path. Therefore, details of the crack growth were first determined using the positional AE amplitude method of Romhány *et al.*[24]

The outcome of this procedure is shown in the example of a SEN-T specimen of the $E+40$ wt-% jute composite (cf. Fig. 9). To represent the centre of gravity of the AE amplitude distribution at a given loading, a Weibull type function was given

$$f_B = A-(A-a_0)\exp\left[-(Bx)^C\right] \tag{3}$$

the J integral is a composed term

$$J = J_e + J_p \tag{4}$$

$$J_e = \frac{\eta_e U_e}{B(W-a)} \tag{5}$$

$$J_p = \frac{\eta_p U_p}{B(W-a)} \tag{6}$$

where J_e and J_p are the elastic and plastic components of the total J value respectively; U_e and U_p are the elastic and plastic components of the external work respectively; η_e and η_p are the elastic and plastic work factors dependent on the specimen geometry respectively; W is the width, B the thickness of the SEN-T loaded specimen and a the actual crack length. The elastic and plastic work factors for the SEN-T geometry were calculated using[24,33]

$$\eta_e = \frac{(W-a_0)\,Y^2(a_0)a_0}{\int_0^{a_0} Y^2(a)a\,\mathrm{d}\,a+(ZW/2)} \tag{7}$$

$$\eta_p = \frac{W-a_0}{W\alpha(a_0)\left\{\frac{W-a_0}{W[\alpha(a_0)-(a_0/W)]}+1\right\}^{-1}} \tag{8}$$

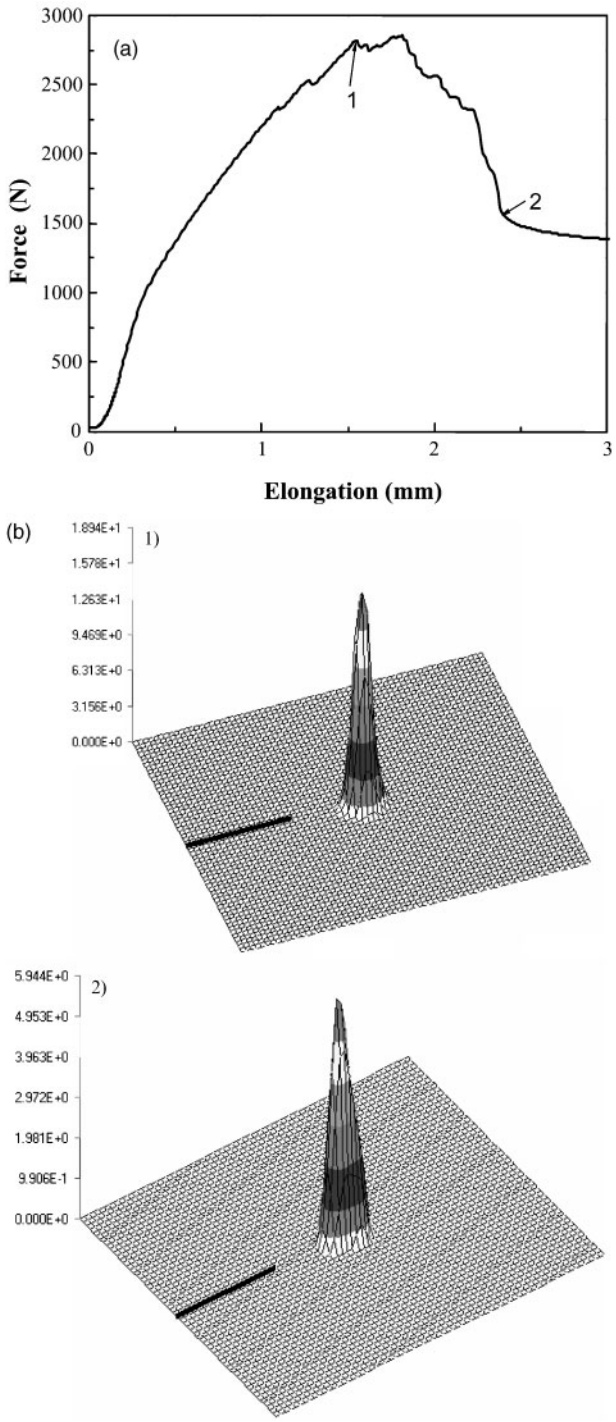

5 *a* characteristic force–elongation curve of SEN-T loaded specimen of composite with 20 wt-% jute cloth and *b* 3D contour plot showing cumulative AE amplitudes registered until load positions were indicated: *z* axis unit is dB mm^{-2} and width of located section of specimen is 50 mm (cf. Fig. 1)

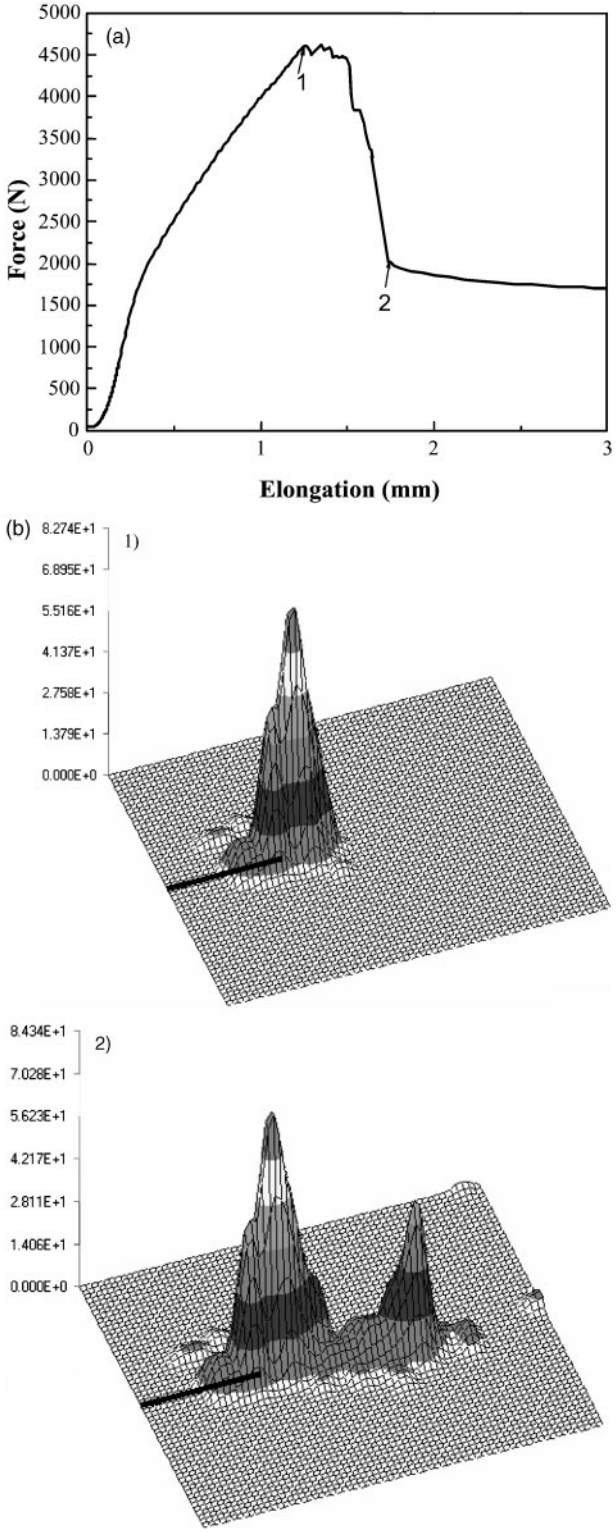

6 *a* characteristic force–elongation curve of SEN-T loaded specimen of composite with 40 wt-% jute cloth and *b* 3D contour plot showing cumulative AE amplitudes registered until load positions were indicated: *z* axis unit is dB mm^{-2} and width of located section of specimen is 50 mm (cf. Fig. 1)

where

$$\alpha = \left[1 - 2\frac{a_0}{W} + 2\left(\frac{a_0}{W}\right)^2\right]^{1/2} \tag{9}$$

$$Y = 1{\cdot}99 - 0{\cdot}41\left(\frac{a}{W}\right) + 18{\cdot}7\left(\frac{a}{W}\right)^2 - 38{\cdot}48\left(\frac{a}{W}\right)^3 + 53{\cdot}84\left(\frac{a}{W}\right)^4 \tag{10}$$

During loading of the SEN-T loaded specimen, the external work performed is partly stored elastically (U_e) and partly consumed by plastic deformation (U_p). To compute the J integral in a given point of the loading (F_i – cf. Fig. 10), the overall area under the curve was

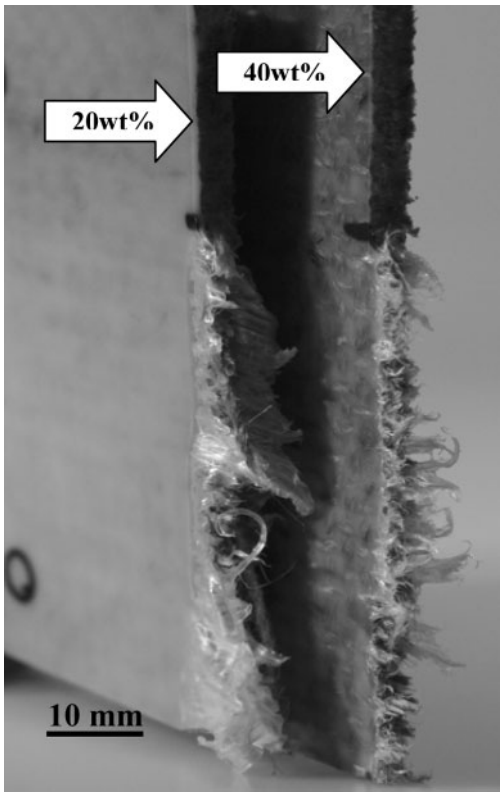

7 Broken SEN-T loaded specimens of composites with 20 and 40 wt-% jute cloth reinforcements respectively

partitioned between *U*p and *U*e as depicted schematically in Fig. 10.

The *J*–*R* curves, constructed from the known values of *J* and Δa, are displayed in Fig. 11. From *J*–*R* curves two parameters are usually read: critical *J* integral value and tearing modulus. Different methods are employed to determine the critical *J* integral, dependant on whether or not the crack tip blunting process is considered. In the present work, the intersection of the linear part of the *J*–*R* curve with the *y* axis (J_0 at $\Delta a=0$) is considered as critical value. Accordingly, the following linear relationship holds

$$J = J_0 + \frac{\Delta J}{\Delta a}\Delta a \tag{11}$$

where $\Delta J/\Delta a$ is the slope/tearing modulus.

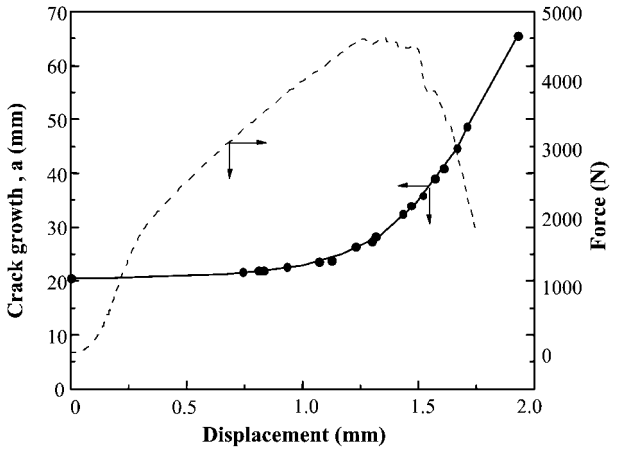

9 Force–displacement curve of crack tip movement along free ligament for SEN-T loaded specimen of *E*+40 wt-% jute cloth

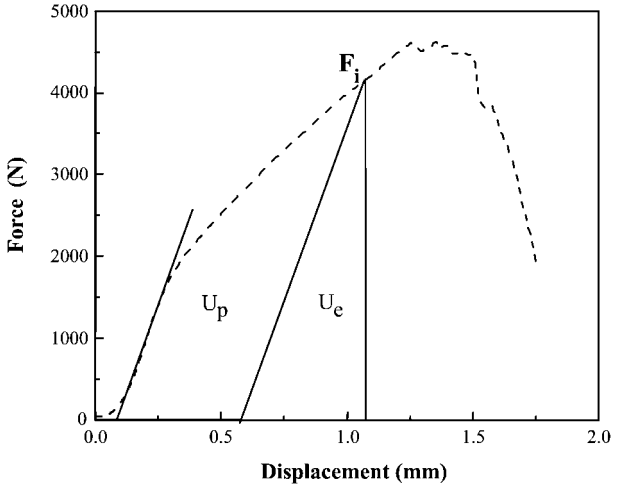

10 Determination of U_p and U_e schematically

Note that the higher J_0 and $\Delta J/\Delta a$, the higher the resistance of the material to crack growth and crack propagation respectively.

Figure 11 shows that with increasing jute content, both J_0 and $\Delta J/\Delta a$ are improved. The related data are: $J_0=27{\cdot}7$ and $34{\cdot}5$ kJ m^{-2}, and tearing modulus $\Delta J/\Delta a=2{\cdot}64$ and $4{\cdot}42$ MJ m^{-3} for the $E+20$ wt-% and

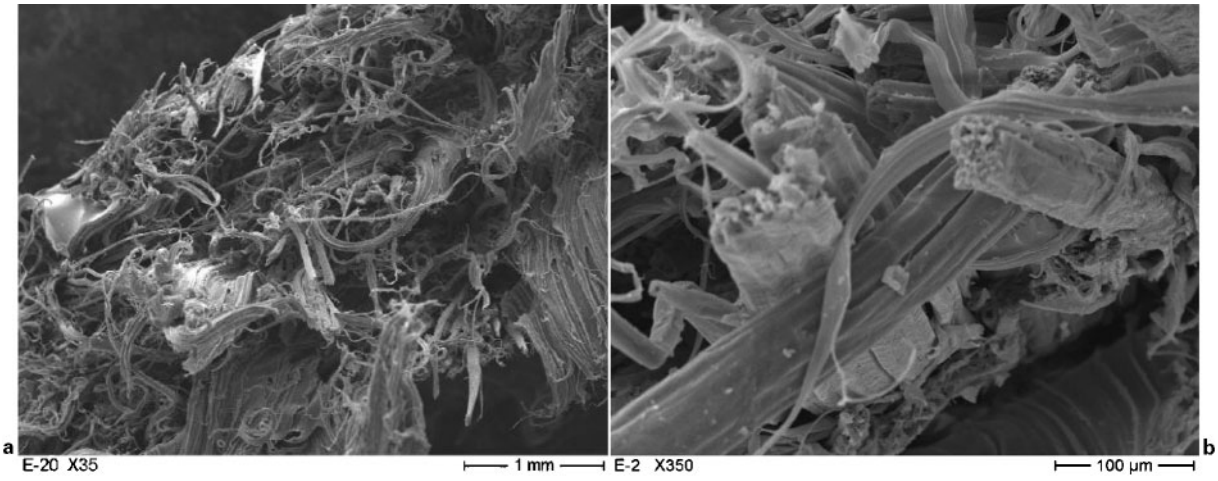

a ×35; *b* ×350

8 Scanning electron microscopy pictures at various magnifications taken from fracture surface of SEN-T specimen with 20 wt-% jute content

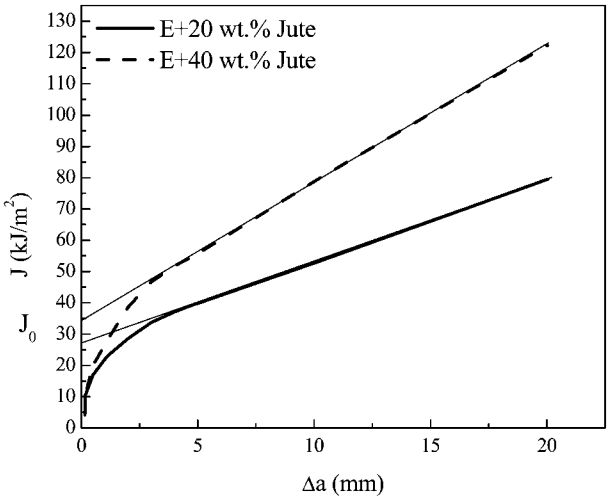

11 J–R curves of composites at 20 and 40 wt-% jute contents respectively

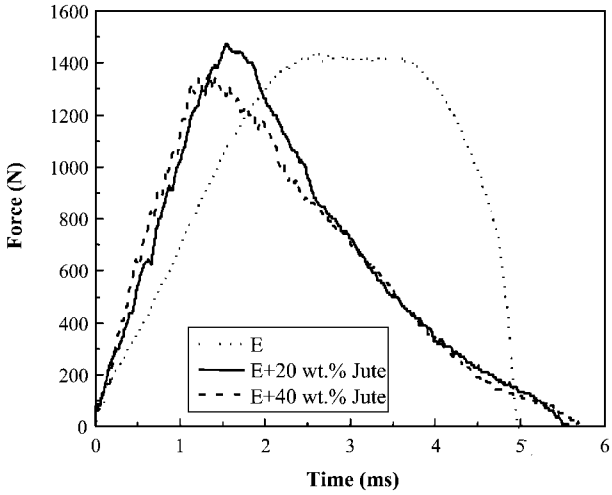

12 Impact (force–time) curves for pure matrix and its composites with 20 and 40 wt-% jute reinforcements at room temperature: impacted sheets have different thicknesses

$E+40$ wt-% jute composites respectively. Note that a simultaneous increase in both parameters is rare.

Out of plane response

Instrumented falling weight impact

Figure 12 shows the characteristic force–time traces registered for the plain matrix and its composites at room temperature. It can be seen that incorporation of jute cloth does not enhance the IFWI resistance compared with the matrix. A similar conclusion can be drawn when collating the fractograms monitored at $T=-30$ and 80°C respectively. Table 3 summarises the IFWI data.

Based on the results in Table 3, it can be concluded that the specific perforation energy was markedly reduced for the composites compared with the matrix at all test temperatures. This 'weakening' effect is in contrast with the reinforcing effect noted for in plane loading. Furthermore, hardly any difference can be found for the composites containing 20 and 40 wt-% jute cloth. The unexpected poor IFWI behaviour of the composites can be attributed to the similar behaviour of the jute cloth. The cloth disintegrates easily because its mesh size is too large to ensure efficient stress transfer to neighbouring meshes in the stressed state, especially under transverse high speed impact.

Failure behaviour

Macrographs of the bottom part of the impacted plates are shown as a function of temperature and jute content in Fig. 13. The matrix failed by breaking the dart induced cusp at −30°C whereas its stretching along the dart circumference was the reason for failure at room temperature. This difference in the failure mode is reflected by the related data in Table 3. The composite failure mode was the same at both −30°C and ambient temperature (as would be anticipated from the related data in Table 3), namely crossed splitting. As noted above, this mode is favoured by the characteristics of the jute cloth.

Conclusions

Based on the present work focusing on the fracture and failure behaviour of jute cloth reinforced biodegradable copolyester (Ecoflex) composites under different mechanical loading modes (in plane and out of plane), the following conclusions can be drawn.

1. Jute cloth is an efficient reinforcement for copolyester matrix for in plane type loading although less useful for high speed out of plane one. This was traced mostly to characteristics of the jute fibre and cloth hampering the stress redistribution in the composite, at least in high frequency tests.

2. Monitoring and locating the AE during static in plane loading helped us to estimate the damage zone and its change along the free ligament of the SEN-T loaded specimens. The size of the damage zone increased with increasing jute content. This was accompanied by increased resistance during crack propagation. The above effect could be quantified by the characteristics of the J–R curves. Both J_0 and the tearing modulus $\Delta J/\Delta a$ increased with increasing jute cloth content. To

Table 3 IFWI impact result

Designation	Test temperature, °C	F_{max}/t, N mm^{-1}	E_{perf}/t, J mm^{-1}	DI
	−30	1295·4±27·0	19·3±0·3	41·5±0·8
E	Room temperature	607·9±15·7	9·7±0·3	54·6±0·8
	80	404·5±4·8	11·0±0·0	13·9±0·8
	−30	546·1±7·5	5·9±0·0	65·6±4·3
E+20 wt-%	Room temperature	488·6±4·2	5·4±0·2	65·9±3·7
	80	383·0±0·9	4·4±0·3	58·0±1·6
	−30	472·2±17·1	6·0±0·2	73·7±0·2
E+40 wt-%	Room temperature	485·6±5·2	5·6±0·1	71·6±2·7
	80	406·9±5·7	4·4±0·2	58·0±2·0

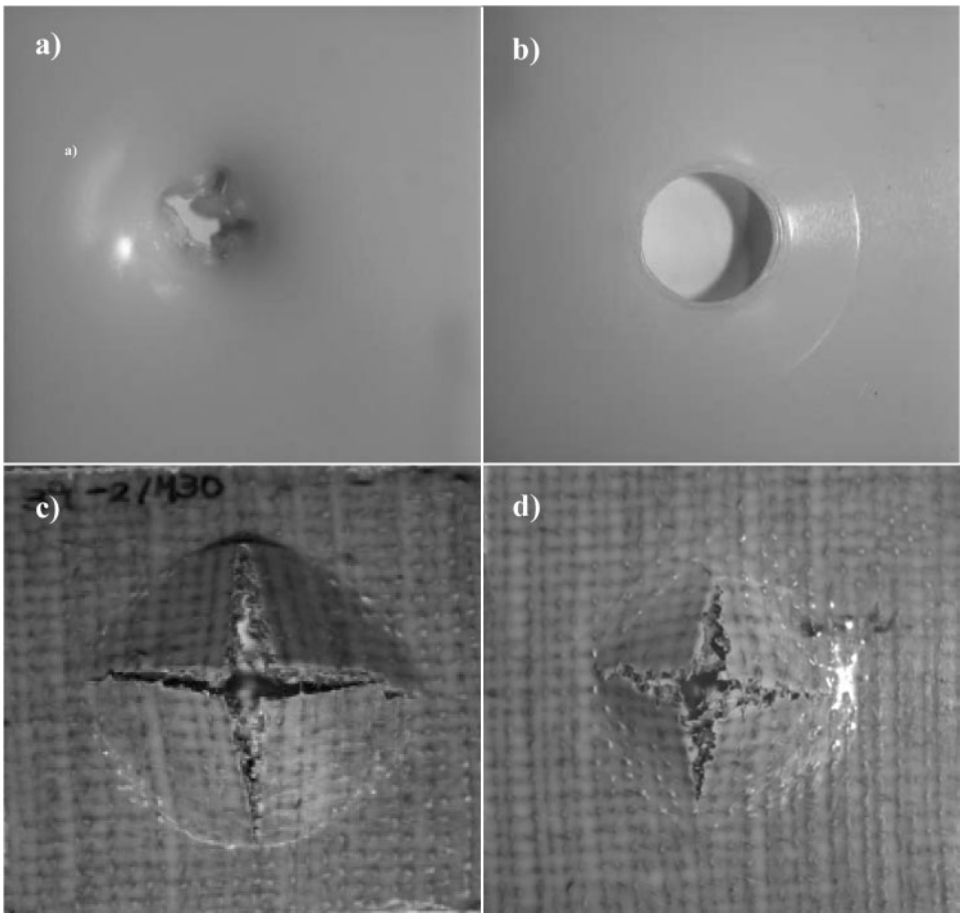

a Ecoflex, −30°C; *b* Ecoflex, RT; *c* *E*+40 wt-% jute, −30°C; *d* *E*+40 wt-% jute, RT

13 Microphotographs of perforated neat Ecoflex and its composite with 40 wt-% jute content (bottom view, i.e. opposite side of impact)

construct the *J*–*R* curves, the crack growth Δa along the ligament was reconstructed by considering the located AE amplitudes.

Acknowledgements

B. A. Acha would like to thank the German Academic Exchange Service (DAAD) for granting her a fellowship for the research conducted at the IVW (Institut für Verbundwerkstoffe GmbH, Germany). The authors are grateful to BASF for their donation of Ecoflex.

References

1. M. Heyde: *Polym. Degrad. Stabil.*, 1998, **59**, 3–10.
2. S. Mishra, A. K. Mohanty, L. T. Drzal, M. Misra and G. Hinrichsen: *Macromol. Mater. Eng.*, 2004, **289**, 955–974.
3. J. Gassan and A. K. Bledzki: *Composites Part A*, 1997, **28A**, 1001–1005.
4. J. M. Felix and P. Gatenholm: *J. Appl. Polym. Sci.*, 1991, **42**, 609–620.
5. P. Gatenholm, J. Kubát and A. Mathiasson: *J. Appl. Polym. Sci.*, 1992, **45**, 1667–1677.
6. B. A. Acha, M. I. Aranguren, N. E. Marcovich and M. M. Reboredo: *Polym. Eng. Sci.*, 2003, **43**, 999–1010.
7. A. K. Bledzki, S. Reihmane and J. Gassan: *Polym. Plast. Technol. Eng.*, 1998, **37**, 451–468.
8. J. Rout, M. Misra, S. S. Tripathy, S. K. Nayak and A. K. Mahanty: *Polym. Compos.*, 2001, **22**, 770–778.
9. S. R. Ranganathan and P. K. Pal: *Pop. Plast.*, 1986, **31**, 29–31.
10. P. Ghosh and P. K. Ganguly: *Plast. Rub. Compos. Process. Appl.*, 1993, **20**, (3), 171–177.
11. P. J. Rao and M. P. Ansell: *J. Mater. Sci.*, 1985, **20**, 4015.
12. A. C. Karmaker and J. Youngquist: *J. Appl. Polym. Sci.*, 1996, **62**, 1147–1151.
13. J. Gassan and A. K. Bledzki: *Polym. Compos.*, 1997, **18**, 179–184.
14. J. Gassan and A. K. Bledzki: *Compos. Sci. Technol.*, 1999, **59**, 1303–1309.
15. M. Gowda, A. C. B. Naidu and T. Rajput Chhaya: *Composites Part A*, 1999, **30A**, 277–284.
16. H. K. Mishra, B. N. Dash, S. S. Tripathy and B. N. Padhi: *Polym. Plast. Technol. Eng.*, 2000, **39**, 187–198.
17. A. K. Rana, A. Mandal, B. C. Mitra, R. Jacobson, R. Rowell and A. N. Banerjee: *J. Appl. Polym. Sci.*, 1998, **69**, 329–338.
18. J. Gassan and A. K. Bledzki: *Composites Part A*, 1997, **28A**, 1001–1005.
19. A. K. Mohanty and M. Misra: *Polym. Plast. Technol. Eng.*, 1995, **34**, (5), 729–792.
20. A. K. Mohanty, M. Misra and G. Hinrichsen: *Macromol. Mater. Eng.*, 2000, **276/277**, 1–24.
21. M. A. Khan, K. M. I. Ali, G. Hinrichsen, C. Kopp and S. Kropke: *Polym. Plast. Technol. Eng.*, 1999, **38**, (1), 99–112.
22. J. Karger-Kocsis: *Adv. Compos. Lett.*, 1998, **2**, 39–43.
23. J. Karger-Kocsis and T. Czigány: *Polym. Polym. Compos.*, 1993, **1**, (5), 329–339.
24. G. Romhány, T. Czigány and J. Karger-Kocsis: *Compos. Sci. Technol.*, 2006, to be published..
25. S. Velayudhana, P. Rameshb, H. K. Varmab and K. Friedrich: *Mater. Chem. Phys.*, 2004, **89**, 454–460.
26. S. N. Nazhat, R. Joseph, M. Wang, R. Smith, K. E. Tanner and W. Bonfield: *J. Mater. Sci. Mater. Med.*, 2000, **11**, 621–628.
27. B. Wielage, T. Lampke, H. Utschick and F. Soergel: *J. Mater. Process. Technol.*, 2003, **139**, 140–146.
28. L. A. Pothan, Z. Oommen and S. Thomas: *Compos. Sci. Technol.*, 2003, **63**, 283–293.
29. P. V. Joseph, G. Mathew, K. Joseph, G. Groeninckx and S. Thomas: *Composites Part A*, 2003, **34A**, 275–290.

30. J. K. Tan, T. Kitano and T. J. Hatakeyama: *J. Mater. Sci.*, 1990, **25**, 3380–3384.
31. J. I. Velasco, C. Morhain, A. B. Martínez, M. A. Rodríguez-Pérez and J. A. de Saja: *Polymer*, 2002, **43**, 6813–6819
32. J. Karger-Kocsis, T. Harmia and T. Czigány: *Compos. Sci. Technol.*, 1995, **54**, 287–298.
33. A. Arkhireyeva and S. Hashemi: *Plast. Rub. Compos.*, 2001, **30**, 337–350.